Using Prenucleation To Control Complex Copolymeric Vesicle Formation in Solution

Xuehao He* and Friederike Schmid

Fakultät für Physik, Universität Bielefeld, D-33615 Bielefeld, Germany

Received September 28, 2006
Revised Manuscript Received November 14, 2006

Vesicles of amphiphilic block copolymers have a large potential in a wide range of applications, e.g., as release systems, carriers or microreactors, or templates for fabricating advanced materials. This is mainly due to the high tunability of the constituent copolymers, more specifically, their chain structure and the selectivity of the monomers.[1] In the past, several morphologies of vesicles have been discovered, such as unilamellar vesicle (ULV),[2] multilamellar or onion-type vesicles (MLV),[3] large compound vesicles (LCV),[4] and others.[5] Different strategies have been used to control the self-assembly and the morphology of vesicles, e.g., changing the interaction between solvent and copolymer or the fraction of different block lengths or mixing different copolymer components. However, it is often difficult to generate vesicles with uniform size and structure in practice. This basic problem comes from the fact that the hydrophilic blocks of the copolymers form a thick corona which prevents vesicles from coalescing. As a result, one usually encounters kinetically stabilized metastable states where vesicles of different size coexist with each other and sometimes even with rodlike or spherelike micelles.

Recently, we have discovered a new mechanism of spontaneous vesicle formation for amphiphilic diblock copolymers in dilute solution,[6] which opens a way out of this dilemma. If a homogeneous solution is quenched into the unstable two-phase region close to spinodal line, vesicles spontaneously form via a pathway which is controlled by nucleation and growth. After an "incubation" time, stable nuclei (micelles) emerge rather suddenly, which then grow steadily into vesicles until almost all copolymers in solution are exhausted. The average final size of vesicles is determined by the number density of these nuclei. In an initially homogeneous solution, the latter is controlled by the wavelength of the spinodal fluctuations. However, we have shown that it can also be imposed, i.e., the system can be *seeded* with micelles, and this will lead to an assembly of largely monodisperse vesicles.[6]

In the present paper, we explore the potential of this "prenucleation" strategy. We find that the number density of seeds c_{ini} can be used to control not only the size of vesicles but also their shape. Depending on c_{ini} and the solubility of the solvent-philic copolymer blocks, complex vesicles with multiple compartments may form, and the number and arrangement of these compartments depend on c_{ini}. Similar structures can be obtained by quenching copolymer nanodroplets of well-defined size.[7] Prenucleation provides an alternative way of control.

We use external potential dynamics (EPD)[8] to test the method in two-dimensional space. Compared with conventional particle simulation methods, field-based methods like EPD have high computational efficiency. Moreover, EPD locally preserves the monomer densities, and the polymer chains have Rouse-type dynamics; hence, the dynamics is nearly realistic on length scales where hydrodynamics are not yet important. The growth of complex vesicles from solution has been studied using field-based simulation methods with nonconserved local densities or local coupling densities.[9] Such simulations are faster compared with EPD. However, we find that the choice of the dynamical model strongly affects the final vesicle morphologies.

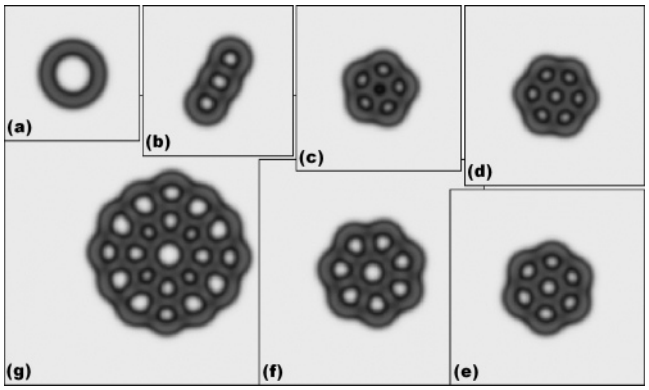

Figure 1. Unilamellar and compound vesicles at various c_{ini} and $\chi_{BS} = 0$. Black and gray stand for solvent-philic and solvent-phobic regions. (a) $c_{ini} = 1.11 \times 10^{-3}R_g^{-2}$; (b) $c_{ini} = 9.0 \times 10^{-4}R_g^{-2}$; (c) $c_{ini} = 7.44 \times 10^{-4}R_g^{-2}$; (d) $c_{ini} = 6.25 \times 10^{-4}R_g^{-2}$; (e) $c_{ini} = 5.33 \times 10^{-4}R_g^{-2}$; (f) $c_{ini} = 4.0 \times 10^{-4}R_g^{-2}$; (g) $c_{ini} = 1.86 \times 10^{-4}R_g^{-2}$.

In the following, all lengths shall be given in units of the mean gyration radius of polymer chains in the unperturbed state, R_g. In order to construct the prenucleation condition, one sphere micelle of radius R_g with a polymer concentration of 0.4 was put at the center of a square simulation box with periodic boundary conditions. The box size L determines the number density of nuclei c_{ini}, $c_{ini} = 1/L^2$. We have studied boxes with sizes L between $16.7R_g$ and $73.3R_g$, which corresponds to values of c_{ini} ranging from $3.6 \times 10^{-3}R_g^{-2}$ to $1.86 \times 10^{-4}R_g^{-2}$. The parameters were chosen as in ref 6: The total volume fraction of amphiphilic diblock copolymer including the initial sphere micelle, f_p, was 10%; the total chain length was $N = 17$, with a solvent-philic fraction of 11.8%. The Flory−Huggins parameters, $\chi_{AB} = 1.05$, $\chi_{AS} = 1.2$, and χ_{BS}, reflect the interaction strengths between two components A (solvent-phobic), B (solvent-philic), and S (solvent), respectively.

As long as the nuclei density c_{ini} is not too low, i.e., $3.6 \times 10^{-3}R_g^{-2} \geq c_{ini} \geq 1.11 \times 10^{-3}R_g^{-2}$, unilamellar vesicles are formed. Because of the bending of the lamella, the concentration of the solvent-philic monomers at the inner layer is always larger than at the outer layer, and it becomes smaller with increasing vesicle size, i.e., decreasing c_{ini}. The dynamical process of self-assembly is essentially identical to that described in ref 6. The average size of vesicles can be estimated directly. Assuming that the thickness of the surrounding lamellae and the monomer density inside the lamellae do not depend on the vesicle size R_v, one obtains a simple scaling relation with c_{ini}: $R_v \sim c_{ini}^{-1}$ in 2D and $R_v \sim c_{ini}^{-0.5}$ in 3D.

At lower values of c_{ini}, complex vesicles are formed. Their structure depends not only on the density of nuclei but also on the solubility of the solvent-philic block. Figure 1 shows the morphologies obtained for $\chi_{BS} = 0$. In this case, multicompartment vesicles are formed, and the number of compartments in the compound vesicle increases with decreasing c_{ini}. At $c_{ini} = 9.0 \times 10^{-4}R_g^{-2}$, a triplet vesicle with three compartments of equal size is found. If c_{ini} decreases further, more compartments emerge, which are arranged in a rosette-like fashion with one

* Corresponding author. E-mail: xhhe@physik.uni-bielefeld.de.

10.1021/ma0622478 CCC: $33.50
Published on Web 11/30/2006

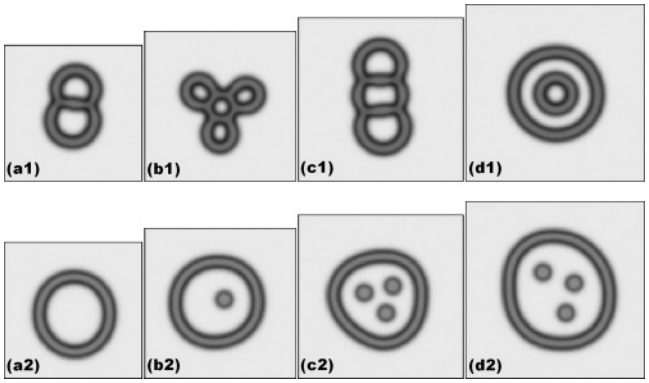

Figure 2. Manifold vesicles at various c_{ini}. Interaction parameters, $\chi_{BS} = -0.3$ (top group), $\chi_{BS} = -0.6$ (bottom group): $c_{ini} = 9.0 \times 10^{-4} R_g^{-2}$ (a1, a2); $c_{ini} = 7.44 \times 10^{-4} R_g^{-2}$ (b1, b2); $c_{ini} = 6.25 \times 10^{-4} R_g^{-2}$ (c1, c2); $c_{ini} = 5.33 \times 10^{-4} R_g^{-2}$ (d1, d2). Black and gray as in Figure 1.

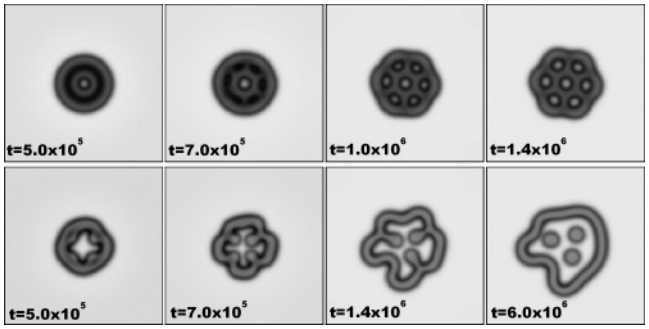

Figure 3. Evolution of morphologies in the intermediate stage for $c_{ini} = 6.25 \times 10^{-4} R_g^{-2}$; $\chi_{BS} = 0$ (top group); $\chi_{BS} = -0.6$ (bottom group). Black and gray as in Figure 1.

compartment in the center and the others distributed symmetrically around it. At very low c_{ini}, a second layer of compartments emerges (Figure 1g).

If we decrease the solubility of the solvent-philic block χ_{BS} from 0 to -0.3, the compartments of the compound vesicle become larger and larger. Novel vesicle structures are discovered (Figure 2, a1−d1). For example, at $c_{ini} = 7.44 \times 10^{-4} R_g^{-2}$, we find a flower-like structure (one central vesicle with three "petals") and at $c_{ini} = 5.33 \times 10^{-4} R_g^{-2}$, a multilamellar structure with two concentric round vesicles. We note that the simulations are reproducible; i.e., the same final structures are usually obtained from different runs with different realizations of the thermal noise.

Hence, the variety of possible vesicle structures increases if one allows for variation of χ_{BS}. If the solubility of the B segment is chosen too large, however, (e.g., $\chi_{BS} = -0.6$, see Figure 2, a2−d2), the complex vesicle morphologies disappear, and one obtains simple unilamellar vesicles with a few embedded sphere micelles. The reasons why solubility differences lead to such dramatically different vesicle morphologies can be understood from analyzing the kinetics of vesicle formation. Figure 3 shows two examples of dynamical evolutions for low and high B solubility. If the B-block is only weakly solvent-philic, $\chi_{BS} = 0$, the local interfacial tension between the lamellar surfaces and the solvent is high, the vesicle walls are stiff, and the vesicles tend to be compact. As a result, the aggregation of copolymers from solution causes the vesicle walls to swell, and they become thicker. Once the thickness of the wall reaches a critical size ($\sim 2R_g$), a fraction of copolymers flip around, and a new layer of solvent-philic B block forms inside the wall. Solvent then diffuses into this layer, and it opens up to give way to multiple hollow compartments (Figure 3, top group). To our knowledge, this is a new mechanism for the formation of large compound vesicles, which differs from the conventional mechanism based on the coalescence of many small vesicles that has been proposed in the past.

The situation is different for strongly solvent-philic B blocks, $\chi_{BS} = -0.6$. In that case, the local interfacial tension between the lamellae and the solvent is low, and the vesicle walls are sloppy. They adjust to copolymer aggregation not by swelling, but by increasing their total area, by fluctuating and wiggling around. The fluctuations become so strong that micelles are eventually cut off and released into the inside of the vesicle. After all copolymers are consumed, the lamellar area no longer increases, but solvent still diffuses into the vesicles such that they finally assume a round shape.

In summary, we have proposed a prenucleation technique to control the vesicle self-assembly after a temperature quench and tested it with EPD simulations of a system that was quenched into a region that is unstable with respect to copolymer−solvent demixing. Unilamellar vesicles were obtained at moderate nuclei densities c_{ini}, and their size can be related to c_{ini}. At low values of c_{ini}, a rich spectrum of large complex compound vesicles was discovered, including twin or triplet vesicles, entrapped vesicles, and vesicle with embedded sphere micelles. The shapes and morphologies of the vesicles were shown to result from the dynamical competition of macroaggregation and microphase separation, and they not only depend on the interaction parameters but also are controlled by c_{ini}. The prenucleation method provides a new way to control the size and structure of self-assembled vesicles, which should be useful for applications. The technique can easily be extended, e.g., by mixing colloidal particle to the solution, or adding non-sphere-like micelles as prenucleation germs. In the future, it will be interesting to extend the analysis to three dimensions. We expect that the basic mechanisms that have been described in this work and that lead to new structures will still be present in 3D. However, more factors will compete with each other (e.g., edges have a line tension, additional point junctions may emerge, etc.), such that the spectrum of possible pathways and final morphologies should become much richer.

Acknowledgment. We gratefully acknowledge the Alexander von Humboldt Foundation for a research fellowship and computational support from PC2 at the Universität Paderborn.

Supporting Information Available: A description of the simulation technique (EPD) and movies showing vesicle self-assembly. This material is available free of charge via the Internet at http://pubs.acs.org.

References and Notes

(1) (a) Hubert, D. H. W.; Jung, M.; German, A. L. *Adv. Mater.* **2000**, *12*, 1291. (b) Zhou, S. Q.; Burger, C.; Chu, B.; Sawamura, M.; Nagahama, N.; Toganoh, M.; Hackler, U. E.; Isobe, H.; Nakamura, E. *Science* **2001**, *291*, 1944. (c) Discher, D. E.; Eisenberg, A. *Science* **2002**, *297*, 967. (d) Antonietti, M, Forster, S. *Adv. Mater.* **2003**, *15*, 1323. (e) Shi, Q.; Wang, J.; Wyrsta, M. D.; Stucky, G. D. *J. Am. Chem. Soc.* **2005**, *127*, 10154.

(2) (a) Zhang, L. F.; Eisenberg, A. *Science* **1995**, *268*, 1728. (b) Discher, B. M.; Won, Y. Y.; Ege, D. S.; Lee, J. C. M.; Bates, F. S.; Disher, D. E.; Hammer, D. A. *Science* **1999**, *284*, 1143. (c) Li, Z. B.; Hillmyer, M. A.; Lodge, T. P. *Nano Lett.* **2006**, *6*, 1245. (d) Lee, J. H.; Agarwal, V.; Bose, A.; Payne, G. F.; Raghavan, S. R. *Phys. Rev. Lett.* **2006**, *96*, 048102.

(3) (a) Shen, H.; Eisenberg, A. *Angew. Chem., Int. Ed.* **2000**, *39*, 3310. (b) Zipfel, J.; Berghausen, J.; Schmidt, G.; Lindner, P.; Alexandridis, P.; Richtering, W. *Macromolecules* **2002**, *35*, 4064. (c) Norman, A. I.; Ho, D. L.; Lee, J. H.; Karim, A. *J. Phys. Chem. B* **2006**, *110*, 62.

(4) (a) Zhang, L. F.; Eisenberg, A. *Macromolecules* **1996**, *29*, 8805. (b) Zhang, L. F.; Yu, K.; Eisenberg, A. *Science* **1996**, *272*, 1777. (c) Du, J. Z.; Chen, Y. M. *Angew. Chem.* **2004**, *116*, 5194.
(5) (a) Yu, K.; Bartels, C.; Eisenberg, A. *Langmuir* **1999**, *15*, 7157. (b) Yu, K.; Eisenberg, A. *Macromolecules* **1998**, *31*, 3509. (c) He, Y. Y.; Li, Z. B.; Simone, P.; Lodge, T. P. *J. Am. Chem. Soc.* **2006**, *128*, 2745.
(6) He, X. H.; Schmid, F. *Macromolecules* **2006**, *39*, 2654.
(7) Fraaije, J. G. E. M.; Sevink, G. J. A. *Macromolecules* **2003**, *36*, 7891.
(8) Maurits, N. M.; Fraaije, J. G. E. M. *J. Chem. Phys.* **1997**, *107*, 5879.
(9) (a) He, X. H.; Liang, H. J.; Huang, L.; Pan, C. Y. *J. Phys. Chem. B* **2004**, *108*, 1731. (b) Sevink, G. J. A.; Zvelindovsky, A. V. *Macromolecules* **2005**, *38*, 7502.

MA0622478